Optimization of capacitive membrane sensors for surface-stress-based measurements

Sajadi, Banafsheh; Goosen, Hans; van Keulen, Fred

Citation (APA)
Sajadi, B., Goosen, H., & van Keulen, F. (2017). Optimization of capacitive membrane sensors for surface-stress-based measurements. *IEEE Sensors Journal*, *17*(10), 3012-3021.
https://doi.org/10.1109/JSEN.2017.2687045

Important note
To cite this publication, please use the final published version (if applicable).
Please check the document version above.

Optimization of Capacitive Membrane Sensors for Surface-Stress Based Measurements

Banafsheh Sajadi, Hans Goosen, Fred van Keulen

Abstract—Surface stress based measurement is a relatively new mechanism in biological and chemical sensing. The viability of this mechanism depends on the maximum sensitivity, accuracy and precision that can be achieved with these sensors. In this paper, an analytical approximate solution and a finite element model are employed to describe the electromechanical behavior of a surface stress based sensor with capacitive measurements. In the proposed model, a circular membrane is assumed as the sensing component, while only a smaller concentric circular area of its surface is subjected to a change in surface stress. The presented approximate analytical solution has a good correspondence with the finite element model and is computationally fast and accurate enough to be an effective design tool. Based on this modeling study, we can determine the optimum design of the sensor to obtain the maximum capacitive sensitivity. Moreover, we study the effect of this optimization on the precision of the system in surface stress sensing. This study shows that the ratio of sensing area to the whole membrane plays a key role in the overall performance of such a sensor.

Index Terms—Surface stress, Capacitive measurements, Micro-membrane, Stoney's formula, Sensitivity, Optimization, Precision.

I. INTRODUCTION

The principle of bio-molecular recognition in nano-mechanical sensors is based on molecular adsorption on one side of a plate-like component [1], [2]. As a consequence, the surface stress of the component changes and this leads to deformation of the component. Next, the corresponding deflection of the system can be measured and used to estimate the surface stress and, thus, the amount of molecular adsorption.

Several types of nano-mechanical components, including cantilevers, doubly clamped beams and membranes, are used for biological detection [1], [3], [4]. Cantilevers are the most commonly used structures in surface stress based measurements. They are highly compliant as compared to other types of structures and their micro-fabrication technology is well established and simpler than for membranes [2], [5]. However, when used in liquid environments, cantilever structures may restrain most types of readout techniques. For example, an electrolyte

The authors are from Structural Optimization and Mechanics Section, Department of Precision and Microsystem Engineering, Delft University of Technology, The Netherlands
Corresponding author: b.sajadi@tudelft.nl

solution around the cantilever allows for Faradic currents which limit most electric readout techniques. In addition, due to the high compliance of cantilevers, even a small flow can affect the cantilever's deflection to a large extent [6], [7].

Clamped plates and membranes, on the other hand, can provide a separation between their detection and sensing surfaces. Thus, in liquid environments, they potentially benefit from a wider range of electric readout techniques [7], [8]. However, compared to cantilevers, a clamped plate is a relatively stiff structure.This structural stiffness results from the boundary conditions which restrict both the transverse displacement and its derivatives at the edges. Particularly, in case of a uniform surface stress loading, it does not show any deformation, and this leads to a poor sensitivity of the overall sensor [5], [9]. In order to narrow this drawback and to maximize the sensing signal, the structural parameters of the sensor should be optimized. The design freedom in such an optimization is mainly restricted to the dimensions of the plate, the shape and dimensions of the functionalized area.

Based on finite elements simulations, it has been shown that the output signal of surface stress based capacitive sensors can be improved by adjusting the geometrical parameters such as the gap between the electrodes and specially, the size of the sensing or functionalized area [10]–[12]. However, the finite element simulations are only valid for specific choices of materials and dimensions, and they do not provide any insight to the problem. In addition, they are generally time-consuming, expensive. On the other hand, an analytical solution —if available— can provide a closed form formulation for calculating the sensitivity of a sensor with any dimension or material. Therefore, analytical solutions are usually preferred for design purposes. In addition, an analytical solution provides more insight to the mechanics of the device, which is paramount for its further development. To the best of our knowledge, no analytical solution is available for calculating the deflection of a fully clamped plate/membrane arising from surface stress changes on a part of its surface.

Apart from the sensitivity, there are some other parameters which have to be considered when evaluating the suitability of a sensor, such as linearity, repeatability,

accuracy and precision. Accuracy is the degree of closeness of a measured or calculated quantity to its reference (expected) value. Accuracy is closely related to precision also called reproducibility. In general, in biological detections, the poor surface coverage of target molecules on the functionalized area (e.g. due to contamination of the surface or poor adhesion), might result in a low accuracy and precision [13]–[16].

It is commonly assumed that if the surface coverage is uniformly dispersed, the surface stress induced by the adsorption exhibits a non-linear dependence on the surface coverage, and it steeply increases when the coverage is near saturation [1], [17], [18]. However, at low concentration of target molecules, or when the target molecules or proteins are large, the distribution of the coverage might be randomly dispersed or just accumulated in one area [18], [19]. In which case, the surface coverage is not as uniform, and the theoretical model will not provide an accurate estimate of the concentration. In practice, low precision can be tackled by employing parallel probes in one measurement. However, still a high reliability of individual sensing components is favorable.

This paper aims to find the optimal design of a capacitive surface stress sensor with a circular clamped plate/membrane as its sensing component. First, an analytical solution is presented to calculate the deformation of such a plate due to a change in the surface stress, while this change occurs only on a smaller concentric area of its surface. Using this study, we can find the optimum size of the functionalized area in order to create the maximum deflection.

Next, we present a design for a membrane-based capacitive sensor for surface stress measurements. Using the presented solution, the capacitive sensitivity of this sensor is obtained analytically. Then, to verify the competence of the approximated solution, the results will be compared to a detailed finite element solution. Eventually, we will discuss the optimized sensitivity of the membrane-shape sensors in comparison with cantilevers, and the effects of material and geometrical parameters on this sensitivity.

Moreover, using the finite element model, we study the effect of the shape and position of the agglomeration of target molecules on the ultimate response of these types of sensors. We show that by optimizing the size of the functionalized area, in addition to achieving a better sensitivity, the performance of the sensor with respect to precision can be improved.

II. ANALYTICAL FORMULATION

In micro-mechanical biological and chemical sensing, the bonding of measurand molecules to the functionalized surface of a plate leads to a change in the surface stress and as a result to bending of the plate. The
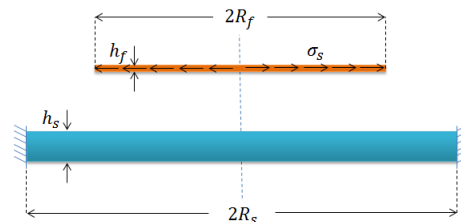

Fig. 1. The thin film and the substrate with different radii, and an equivalent pretension in the thin film

surface stress variation for plate-like structures is usually estimated analytically by applying the famous "Stoney" equation. The latter provides a linear relationship between the tangential surface stress in the surface layer and the curvature of the plate [20]. Stoney's equation, however, was initially derived for a system composed of a pre-stressed thin film attached to and fully-covering a relatively thick substrate with free boundary conditions.

There are many extensions and modifications of Stoney's equation to relax some of its simplifying assumptions [21]–[23]. Yet, this equation has not been extended or modified for a fully-clamped circular plate, up until now. In this section, we shall derive a closed form approximate solution for calculating the deflection of a clamped circular plate due to a change in surface stress on a circular and concentric smaller functionalized area of its surface.

An isotropic and homogeneous clamped circular plate of radius R_s is considered (Figure 1). As a substitute for the functionalized surface layer, a thin film is assumed to be attached to the substrate. The shape of the film is circular and concentric with the substrate. The radius of this film is R_f and it is subjected to a pretension which is equivalent to the change in surface stress . The thickness of the thin film and the substrate are h_f and h_s, respectively, where $\frac{h_f}{h_s} \ll 1$. The Young's modulus and Poisson's ratio of the film and substrate are E_f, ν_f, E_s and ν_s, respectively. The problem is considered to be axisymmetric and Kirchhoff plate theory is employed. In all other parameters to be introduced, the subscripts s and f refer to the substrate and the thin film, respectively.

The chemical reaction between the functionalized surface and the measurand bio-molecules introduces a surface stress to the plate. This tangential surface stress change is modeled with an equivalent tangential stress resultant (σ^s) in the thin film. This stress resultant (σ^s) is assumed to be isotropic, i.e. similar in radial and angular directions, and uniform. In the analysis, we can either consider the tangential stress resultant in the film, or an equivalent isotropic and uniform in-plane strain ε_m. This equivalent strain can be calculated with Hooke's

law giving

$$\varepsilon_m = \sigma^s \frac{1 - \nu_f}{E_f h_f}. \tag{1}$$

If we attach the pre-stressed thin film to the clamped plate, the system will deform to relax the stress in the film. We analyze the equilibrium state of the film and the plate after the relaxation, together as one system.

Let u_f and u_s denote the radial displacements at the mid-plane of the thin film and substrate after relaxation of the system, and w the out-of-plane displacement in both. Since the film is relatively thin, the variation of its displacement and stress components in transverse direction is negligible. The continuity of displacements across the film/substrate interface requires:

$$u_f = u_s - \frac{h_s + h_f}{2} \frac{dw}{dr}. \tag{2}$$

Based on Kirchhoff plate theory, the non-vanishing stress resultant in the thin film and the substrate (N_r and N_θ in radial and tangential directions) can be calculated as:

$$N_{rf} = \frac{E_f h_f}{1 - \nu_f^2} \left(\frac{du_f}{dr} + \nu \frac{u_f}{r} \right) + \sigma^s, \tag{3}$$

$$N_{\theta f} = \frac{E_f h_f}{1 - \nu_f^2} \left(\nu_f \frac{du_f}{dr} + \frac{u_f}{r} \right) + \sigma^s, \tag{4}$$

$$N_{rs} = \frac{E_s h_s}{1 - \nu_s^2} \left(\frac{du_s}{dr} + \nu_s \frac{u_s}{r} \right), \tag{5}$$

$$N_{\theta s} = \frac{E_s h_s}{1 - \nu_s^2} \left(\nu_s \frac{du_s}{dr} + \frac{u_s}{r} \right). \tag{6}$$

The tangential stress couples of the substrate in radial and tangential directions (M_r and M_θ) can be calculated by

$$M_{rs} = \frac{E_s h_s^3}{12(1 - \nu_s^2)} \left(\frac{d^2 w}{dr^2} + \frac{\nu_s}{r} \frac{dw}{dr} \right), \tag{7}$$

$$M_{\theta s} = \frac{E_s h_s^3}{12(1 - \nu_s^2)} \left(\nu_s \frac{d^2 w}{dr^2} + \frac{1}{r} \frac{dw}{dr} \right). \tag{8}$$

If we assume the plate and the film, together, as one laminated plate, the non-vanishing stress resultant in this structure can be calculated for $r < R_f$ and $R_f < r < R_s$, as

$$N_r = \begin{cases} N_{rf} + N_{rs} & r < R_f, \\ N_{rs} & R_f < r, \end{cases} \tag{9}$$

$$N_\theta = \begin{cases} N_{\theta f} + N_{\theta s} & r < R_f, \\ N_{\theta s} & R_f < r. \end{cases} \tag{10}$$

In calculating the tangential stress couples of the system, the equivalent moment due to presence of the thin film should be considered. Hence,

$$M_r = \begin{cases} N_{rf} \frac{h_s + h_f}{2} + M_{rs} & r < R_f \\ M_{rs} & R_f < r, \end{cases} \tag{11}$$
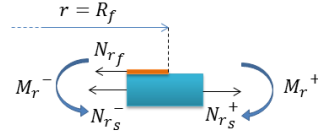

Fig. 2. Cross section of a volume element at the edge of the film, including the thin film and the substrate, and the associated stress resultants and couples.

$$M_\theta = \begin{cases} N_{\theta f} \frac{h_s + h_f}{2} + M_{\theta s} & r < R_f \\ M_{\theta s} & R_f < r. \end{cases} \tag{12}$$

For the laminated plate, the equilibrium in radial and transverse directions can be expressed as [24]:

$$N_r - N_\theta + \frac{dN_r}{dr} r = 0, \tag{13}$$

$$M_r - M_\theta + \frac{dM_r}{dr} r = 0. \tag{14}$$

Using Equations (9)–(14), we obtain:

$$\begin{cases} N_{rf} - N_{\theta f} + \frac{dN_{rf}}{dr} r \\ \quad + N_{rs} - N_{\theta s} + \frac{dN_{rs}}{dr} r = 0 & r < R_f, \\ N_{rs} - N_{\theta s} + \frac{dN_{rs}}{dr} r = 0 & R_f < r, \end{cases} \tag{15}$$

and

$$\begin{cases} \frac{h_s + h_f}{2} (N_{rf} - N_{\theta f} + \frac{dN_{rf}}{dr} r) \\ \quad + M_{rs} - M_{\theta s} + \frac{dM_{rs}}{dr} r = 0 & r < R_f, \\ M_{rs} - M_{\theta s} + \frac{dM_{rs}}{dr} r = 0 & R_f < r. \end{cases} \tag{16}$$

Due to the presence of a discontinuity at $r = R_f$, the equilibrium of forces and moments for a volume element on the edge of the film should be considered separately:

$$N_{rf}^- + N_{rs}^- = N_{rs}^+, \tag{17}$$

and,

$$\frac{1}{2}(h_s + h_f) N_{rf}^- + M_{rs}^- = M_{rs}^+. \tag{18}$$

The superscripts $-$ and $+$ denote the limits of the functions in R_f from $r < R_f$ and $r > R_f$, respectively (see Figure 2). It should be noticed that here, the thin film stress resultant N_{rf} includes the driving load σ^s.

Next, following Equations (2)–(16), the general solutions for the displacement components u_s and w can be calculated. Considering that the displacement should be finite at $r = 0$, the general solution of the equilibrium equations is obtained as:

$$w = \begin{cases} C_1 r^2 + C_2 & r < R_f, \\ C_3 r^2 + C_4 \ln r + C_5 & R_f < r, \end{cases} \tag{19}$$

$$u_s = \begin{cases} C_6 r & r < R_f, \\ C_7 r + C_8/r & R_f < r. \end{cases} \quad (20)$$

The radial displacement in the thin film (u_f) follows from Equation (2). The parameters C_i (i=1–8) are the unknown degrees of freedom to be determined by satisfying continuity and boundary conditions, and the equilibrium at $r = R_f$ as expressed by (17) and (18). Continuity at the edge of the thin film requires:

$$u_s^+ = u_s^-, \quad (21)$$

$$w^+ = w^-, \quad (22)$$

$$\frac{dw}{dr}^+ = \frac{dw}{dr}^-. \quad (23)$$

The clamping boundary condition implies:

$$u_s|_{R_s} = 0, \quad (24)$$

$$w|_{R_s} = 0, \quad (25)$$

$$\frac{dw}{dr}|_{R_s} = 0. \quad (26)$$

Hence, the unknown constants (C_i) can be calculated. Because of their complexity, the resulting expressions are not shown here. If we assume $\frac{h_f}{h_s} \ll 1$, and if the stiffness of the two materials is of the same order of magnitude (thus, higher-order terms of $\frac{E_f}{E_s}\frac{h_f}{h_s}$ can be neglected with respect to 1), the solution for the displacement field can be simplified to:

$$w = \begin{cases} 3\frac{\sigma^s}{h_s^2}\frac{1-\nu_s^2}{E_s}[R_f^2 \ln \frac{R_f}{R_s} \\ \qquad + (1 - \frac{R_f^2}{R_s^2})\frac{r^2}{2}] & r < R_f, \\ \\ 3\frac{\sigma^s}{h_s^2}\frac{1-\nu_s^2}{E_s}[R_f^2 \ln \frac{r}{R_s} \\ \qquad + \frac{R_f^2}{2}(1 - \frac{r^2}{R_s^2})] & R_f < r, \end{cases} \quad (27)$$

$$u_s = \begin{cases} -\frac{1}{2}\frac{\sigma^s}{h_s}\frac{1-\nu_s^2}{E_s}(1 - \frac{R_f^2}{R_s^2})r & r < R_f, \\ \\ -\frac{1}{2}\frac{\sigma^s}{h_s}\frac{1-\nu_s^2}{E_s}(\frac{R_f^2}{r^2} - \frac{R_f^2}{R_s^2})r & R_f < r. \end{cases} \quad (28)$$

The maximum deflection of the system is at $r = 0$ and is equal to

$$\Delta w = 3\frac{\sigma^s}{h_s^2}\frac{1-\nu_s^2}{E_s}R_f^2 \ln \frac{R_f}{R_s}. \quad (29)$$

Equation (29) can be looked upon as an extension of Stoney's formula for a film and substrate with different radii, with clamped boundary condition. Obviously if $R_f \rightarrow 0$, no film is left on the substrate and the deflection equates to zero. Also, if $R_f = R_s$, the deflection of the plate would vanish completely. This suggests the possibility of finding the optimum radius for the functionalized area which leads to the maximum

deflection of the substrate. This, in turn, may provide the maximum sensitivity of the sensors (e.g., based on using optical readout techniques). Clearly, the maximum deflection is achieved when $\frac{\partial w|_{r=0}}{\partial R_f}$=0. By solving this maximization problem, one can show that the optimum ratio of $\frac{R_f}{R_s}$ is always $\frac{R_f}{R_s} = 0.606$, and the corresponding maximum deflection of the membrane (i.e. its absolute amount) would be

$$\Delta w_{max} = \alpha \frac{\sigma^s}{h_s^2}\frac{1-\nu_s^2}{E_s}R_s^2, \quad (30)$$

where $\alpha = 0.552$ (when $\frac{E_f}{E_s}\frac{h_f}{h_s} \ll 1$). This result is comparable to Stoney's solution for deflection of a cantilever due to a change in its tangential surface stress, where the thickness of the cantilever is the same as the membrane and its length is equal to the membrane radius:

$$w_{st} = 3\frac{\sigma^s}{h_s^2}\frac{1-\nu_s}{E_s}R_s^2. \quad (31)$$

Equations 31 and 30 imply the maximum deflection of a membrane, in optimized configuration, would be $0.184(1 + \nu_s)$ times that of an equivalent cantilever. The comparison between the sensitivity of cantilevers and membranes will be discussed in more detail in the Section "Results and discussion".

III. SENSITIVITY OF THE CAPACITIVE MEMBRANE SENSOR

In this section, the sensitivity of a *capacitive* sensor for surface stress based measurements is studied. A simplified model of this sensor with a micro-membrane as its sensing component is considered. A part of its surface is coated with a thin metal layer which, in fact, plays two roles. First, its surface is functionalized with probe molecules to adsorb the target molecules and second, it acts as an electrode for capacitive measurements. The whole structure is suspended over a conductive pad which is the other electrode for capacitance measurements. This conceptual design is graphically shown in Figure 3. The initial capacitance between two straight and parallel electrodes, can be calculated by

$$C_0 = \epsilon_r \epsilon_0 \frac{A_e}{d}, \quad (32)$$

where ϵ_0 is the vacuum permittivity, ϵ_r is the relative permittivity of the material between the plates, A_e is the electrode surface area, and d is the distance between the electrodes. The adsorption of target molecules on the metal layer will create a change in its surface stress which causes the membrane to deflect. After deflection, the capacitance of the system can be calculated by

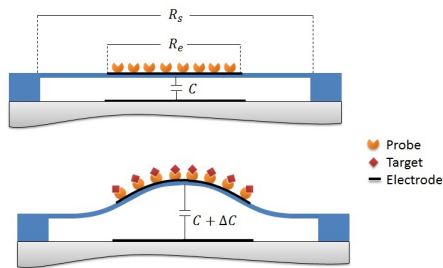$$C = \epsilon_r \epsilon_0 \int \frac{dA_e}{d + w}, \quad (33)$$

Fig. 3. The schematic of the capacitive sensor for surface stress measurement, before (top) and after (bottom) the reaction between the probe and target molecules

where w is the transverse deflection of the thin film (flexible electrode). The *sensitivity* of the sensor is defined as the relative capacity change to the input parameter, i.e., change of surface stress in the functionalized area. Using (32) and (33), the absolute change in capacitance can be calculated by

$$\Delta C = \varepsilon_r \varepsilon_0 \pi \left(\frac{R_e^2}{d} - \int_0^{R_e} \frac{2r\,dr}{d+w} \right), \qquad (34)$$

which can be approximated using the expression for w in Equation (27), and the electrode radius (R_e) can be replaced by the radius of the thin film subjected to the change in surface stress (R_f). If the applied surface stress change (σ^s) is small, the response of the sensor can be linearized and therefore, the sensitivity of the sensor will be proportional to $\Delta C / \sigma^s$.

In order to maximize the sensitivity, the dimensions of the sensor shall be optimized. Clearly, a higher sensitivity can be achieved by decreasing the initial distance between the electrodes (d). However, the electrode radius (R_e) has an optimum size which can be calculated analytically by equating the first derivative of ΔC with respect to R_e (or R_f) to zero:

$$\frac{\partial(\Delta C)}{\partial R_e} = 0. \qquad (35)$$

It should be mentioned that R_e which optimizes the maximum displacement is different from the one which maximizes ΔC. The results of this analysis will be discussed in Section "Results and discussion".

IV. FINITE ELEMENT MODEL

In order to evaluate the accuracy of the presented analytical solution, the simple sensor described in the last section is modeled with finite element software (COMSOL). The membrane is considered to be Silicon (undoped) which is a very common choice for MEMS devices. The electrode is chosen to be gold which is one of the most used materials for immobilizing bio-receptors on nanomechanical systems [1], [9], [10], [25].

The gap between the membrane and the bottom electrode is assumed to be filled with low pressure air. The mechanical properties of the chosen materials and other specifications of the model are given in Table I.

The finite element model is 3D, and the mechanics and electrostatics equations of the system are solved fully coupled. The Silicon membrane and the thin surface layer are discretized with tetrahedral solid elements and triangular shell elements, respectively. The air gap is also discretized with tetrahedral elements to calculate the electrostatic field.

The surface layer of the electrode subjected to the surface stress is modeled with a very thin membrane, and the surface stress is modeled with a an equivalent pretension in this membrane. A pretension of 10 mN/m, which is a typical surface stress caused in biological reactions, is applied to the surface layer. Then, the mechanical and electrical response of the system are calculated. This calculation was performed for different electrode radii. The results of the FEM calculations and the proposed analytical solution will be compared in Section VI.

V. PRECISION OF THE SENSOR

In addition to sensitivity, accuracy and precision are two other sensor parameters which have to be considered in its design. *Precision* refers to the closeness of results of the measurements, for a similar input, to each other. *Accuracy* is the degree to which the average result of the measurement, conforms to the reference (expected) value. These two terms are graphically explained in Figure 4.

In surface stress based measurements, in order to function as a sensor, the concentration of the target molecules must be related to the surface stress, which in turn results in different deflections. As mentioned in the Introduction, a low density of the target molecules in the environment results in a partial coverage of the functionalized surface. Hence, only a part of the functionalized area will be
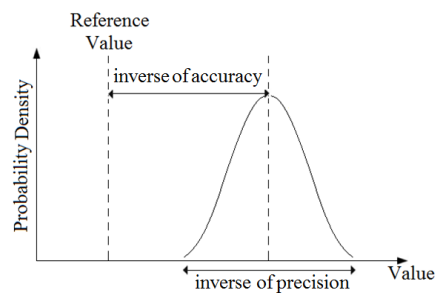

Fig. 4. A graphic definition of accuracy and precision of a sensor.

TABLE I
MODEL PARAMETERS

	Membrane	Electrode	Gap
Material	Silicon	Gold	Air
Elasticity Modulus	169 GPa	80 GPa	
Poisson ratio	0.2	0.3	
Radius	125 μm	R_e	
Thickness	0.5 μm	0.025 μm	2 μm
Relative Permittivity	11.68	1	1.006

subjected to the surface stress change. Let us denote the ratio between this area to the whole functionalized area as *coverage ratio*.

Here, we assume that the coverage ratio increases monotonically with the density of molecules in environment [17], [19]. So, the coverage ratio is equal to 1, if the concentration of target molecules is high enough and the surface is saturated. Otherwise, the coverage ratio is lower than 1.

When the coverage ratio is less than one, it could imply a patch wise covering due to the agglomeration of target molecules in one area. The shape and the position of this agglomeration can influence the ultimate response of the sensor. Therefore, the output signal is not only a function of the coverage ratio, but also its shape, and this accordingly reduces the precision.

In Section II we showed that if the coverage is uniform over the functionalized area, a full size electrode ($R_e = R_s$) will result in very poor sensitivity. However, when a poor coverage is obtained, the size of electrode might seem irrelevant. In this section, we briefly study the effect of the radius of the functionalized area (thin electrode) on the performance of the sensor in case of a partial coverage. For this purpose, two models with different radii of the gold layer, one with maximum sensitivity and one covering the whole membrane, are considered. The finite element model employed is similar to that of the previous section.

The shape of the surface layer (modeled with a thin membrane) mimics the shape of the agglomeration of the molecules. In the finite element model this shape is controlled with a parametrized function as

$$x = X_0 R_e + R_e (\Sigma_{i=0}^n A_i \cos(is)) \cos(s),$$
$$y = R_e (\Sigma_{i=0}^n A_i \cos(is)) \sin(s), \tag{36}$$

where x and y are the Cartesian coordinates and s is a curve parameter from 0 to 2π. As a matter of fact, Equation 36 resembles a Fourier Cosine expansion of the actual shape of the agglomeration of the molecules. The advantage of the Fourier representation is the level-of-detail interpretation which is provided by the parameter i. The low values of this parameter represent the coarse structure of a shape, while higher values add the details. In Equation 36, the parameter X_0 is introduced to move

the created area out of the center. To study the effect of the shape of the adsorption area on the output, this parameter and the parameters A_i (assuming i=1–7) are varied between 0 to 1 randomly. In addition, if the shape intersects with the perimeter of the functionalized area ($\sqrt{x^2 + y^2} > R_f$), only the inner part is subjected to the surface stress change. Any curve intersecting itself is skipped in the simulation, automatically.

Next, similar to the previous section, a pretension of 10 mN/m is applied to the surface layer, and deflection and capacitance of the system are calculated. Figure 5, for example, shows one configuration of this model before and after deformation. Due to different shapes of the adsorption area, a range of capacitance change is obtained for one coverage ratio. In practice, it is desired to restrict the range of the response in order to achieve a better precision in the sensor. Therefore, using the COMSOL model, the effect of the size of
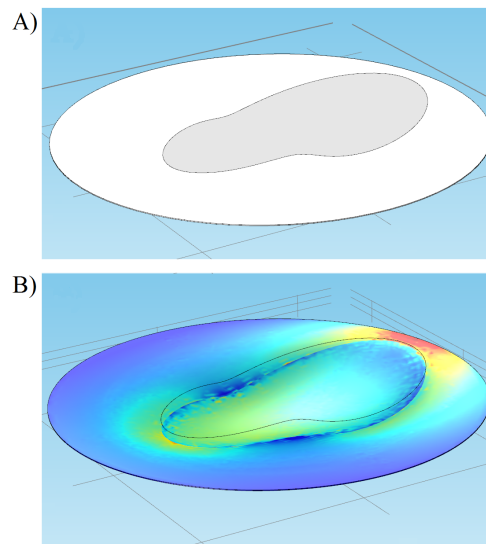

Fig. 5. A part of the Comsol model, including the silicon membrane, the flexible electrode covering the whole membrane, and the thin layer with a random shape mimicking an agglomeration of molecules, A) before deformation, and B) after deformation due to a positive surface stress change.

the functionalized area on the range of the capacitance changes is studied.

As a result of the FEM simulations, two factors of *eccentricity* and *circularity* were found to be appropriate and influential factors, for discussing the shape of the agglomeration of molecules. Circularity (f_c) is commonly used in image analysis and allows us to see how far a shape is from a circle. This shape factor is defined as

$$f_c = \frac{4\pi A}{P^2}, \tag{37}$$

where A is area and P is the perimeter of the related shape. Clearly, this factor is one for a circle and less than one for any other shape. Eccentricity (f_e) is defined as the ratio of the distance between the center of the adsorption area and the center of the plate, to the radius of the functionalized area. The results of this study are presented and discussed in Section VI.

VI. RESULTS AND DISCUSSIONS

To discuss the effect of the size of the functionalized area on the sensitivity of a membrane sensor, we consider the model parameters given in Table I as a test case. Considering that Silicon is a relatively stiff material (see Table I), the simplifying assumption $\frac{E_f}{E_s}\frac{h_f}{h_s} \ll 1$ holds and consequently, the solution for the displacement field is very close to the analytical solution presented by (27) and (28).

Figure 6 shows the deflection for the center of the plate as a function of the radius of the functionalized area (electrode). The graphs in this figure are obtained using the approximate analytical solution and the finite element model. It shows that the results of the two solutions are in close agreement which confirms the accuracy of the presented approximate solution.

It should be noticed that this problem is solved for a small surface stress of 10 mN/m, which does not cause a large deflection. Therefore, the results of the nonlinear finite element model lead to a *slightly* lower deflection compared to the linear approximate solution. Figure 6 clearly shows that the maximum deflection of the membrane occurs when the radius of the electrode is 0.6 of that of the membrane. This optimized radius hardly depends on the choice of parameters, as long as $\frac{E_f}{E_s}\frac{h_f}{h_s} \ll 1$.

Figure 7 shows the change in the capacitance of the sensor as a function of the radius of the functionalized area (electrode). It should be mentioned that in our finite element model, the permittivity of the Silicon membrane and the air gap, and the fringing electric field around the periphery of the electrodes are all included. These factors (particularly the permittivity of the Silicon membrane) cause an absolute difference in capacitance from those predicted analytically. However, the relative
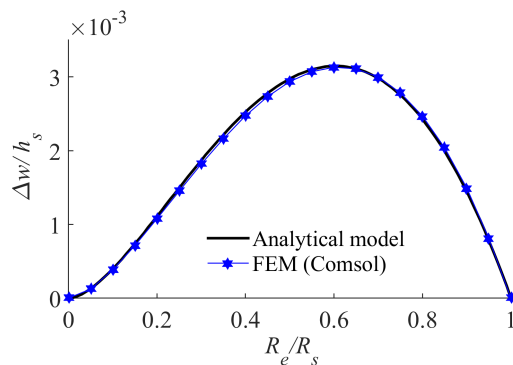

Fig. 6. Deflection of a silicon membrane due to 10 mN/m change in surface stress, as a function of the normalized radius of the functionalized area.
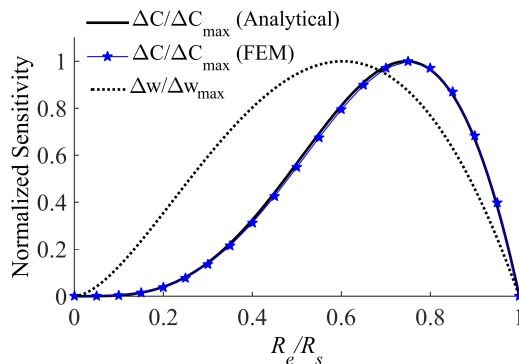

Fig. 7. The normalized capacitance change of the system and maximum deflection of the curvature due to a change in surface stress, as a function of the normalized radius of the functionalized area.

capacitance change is similar for both the FEM and analytical models.

As can be observed from Figure 7, the sensitivity is maximum for an optimum radius of the functionalized area, $R_e/R_s = 0.76$. This optimum radius depends on the choice of the parameters of the sensor, i.e., materials and dimensions of the sensor. In order to compare the effect of the electrode radius on the capacitance and deflection of the system, the normalized deflection of the membrane is also shown in Figure 7. The results clearly show that the optimum radius to maximize the capacitive sensitivity is different from the one which maximizes the deflection.

This analysis was also performed for other choices of materials, while preserving other parameters in Table I. The normalized deflection and the change in capacitance are shown in Figure 8 as a function of the radius of
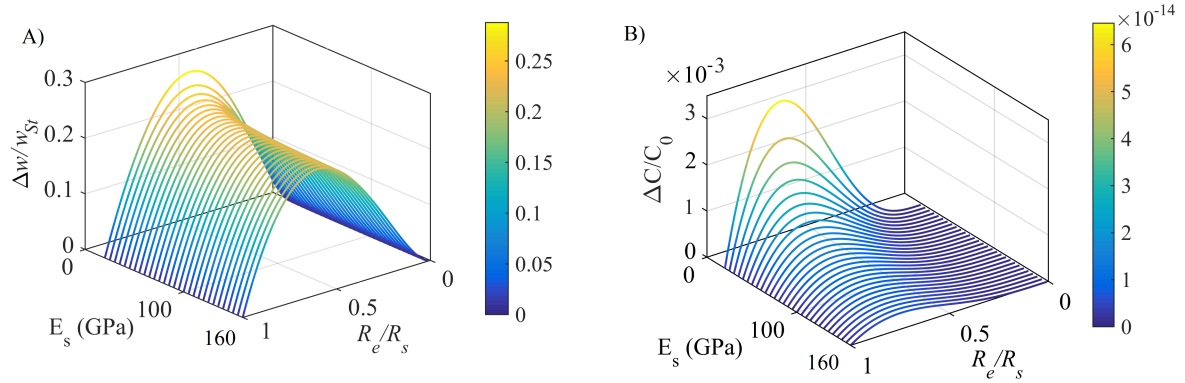
Fig. 8. A) The maximum deflection of a membranes normalized by the deflection of an equivalent cantilever and B) the normalized change of the capacitance of the system due a change in surface stress, vs. Young's modulus of the membrane and the relative radius of functionalized area. The change in capacitance is normalized by (C_0) the capacitance of the system if $R_e = R_s$.

functionalized area and the Young's modulus of the membrane. It should be mentioned that for relatively compliant materials (i.e. smaller E_s), the simplifying assumption $\frac{E_f}{E_s}\frac{h_f}{h_s} \ll 1$ does not hold and hence, the graphs in Figure 8 are obtained by the exact solution of (19)-(26).

Clearly, the sensitivity of a mechanical sensor increases if a more compliant material is employed for the sensing component. This could also be observed from Equation (30). In the current case, however, the optimized size of the functionalized area also depends to E_s, and hence, so does the parameter α in (30). In order to observe this effect, the maximum deflection of the membrane, $\Delta w = w|_{r=0}$, is normalized by the deflection of an equivalent cantilever, as given in (31).

According to Figure 8-A, by optimizing the radius of the functionalized area, the deflection of a clamped membrane can be optimized to a minimum of 22 percent of an equivalent cantilever. For stiff materials, where $E_s > 50$ GPa (e.g. Si, SiO2, SiN), the optimum radius is hardly dependent on the material property and the optimum radius to maximize capacity is $R_e/R_s \approx 0.76$. However, this optimum radius and the maximum achievable deflection significantly differ for more compliant materials (e.g., polymers). For instance, for a Young's modulus of $E_s = 20$ GPa, the optimum radius changes to $R_e/R_s = 0.54$ and the deflection of the clamped membrane can be optimized to 29 percent of an equivalent cantilever.

Figure 8-B shows the change in capacitance of the system as a function of the Young's modulus of the membrane and the radius of the functionalized area. It shows that the maximum capacitive sensitivity, and the associated optimum radius, strongly depend on the

material of the membrane. The overall capacitive sensitivity of the sensor is increased by a factor 10 when the compliance of the membrane is decreased by only a factor 8. In fact, the results shown in Figure 8 imply that this optimization has a better result for materials with lower stiffness.

It should be mentioned here that if the membrane is made of a conductive material (like doped Silicon), the whole membrane serves as an electrode (i.e. $R_e = R_s$). Then, the gold layer will only provide the functionalized surface (i.e. $R_f \neq R_e$). In this case, the optimum radius of the functionalized area (R_f) to create the maximum capacity change will be different and can be calculated based on the solution method proposed in this paper. For such a case using the test parameters at hand, the radius of $R_f/R_s = 0.71$ will maximize the capacitive sensitivity.

It is noteworthy that the other design parameter which has an influence on sensitivity is the slenderness of the membrane ($S = \frac{R_s}{h_s}$). As Equation (30) shows, the deflection of the membrane increases monotonically with the aspect ratio of the membrane. This means that by increasing the slenderness, the sensitivity of the sensor will increase. However, this parameter has no influence on the optimum radius of the electrode for maximizing the sensitivity of the system.

This analysis was performed based on a full coverage of target molecules on the functionalized area and a uniform surface stress change. Next, we discuss how the optimization of the radius of the functionalized area can affect the precision for biological and chemical detections, if the coverage is not full and uniform. Figure 9 shows three differently shaped adsorption areas, though with similar coverage ratios. Although these examples
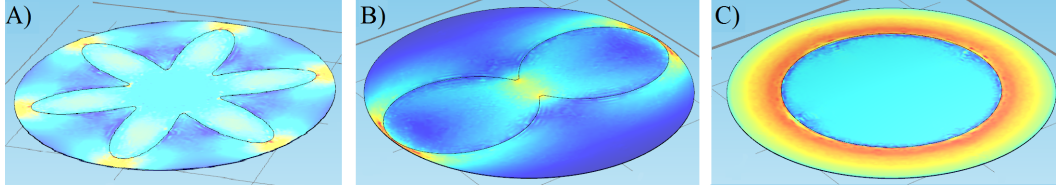
Fig. 9. Three different shape of the surface layer mimicking the agglomeration of molecules on the functionalized area, with a same coverage ratio of 0.45, and different circularity A)$f_c = 0.23$ and $\Delta C/C_{max} = 2.126 \times 10^{-4}$, B)$f_c = 0.52$ and $\Delta C/C_{max} = 1.032 \times 10^{-4}$, c)$f_c = 1$ and $\Delta C/C_{max} = 3.021 \times 10^{-4}$
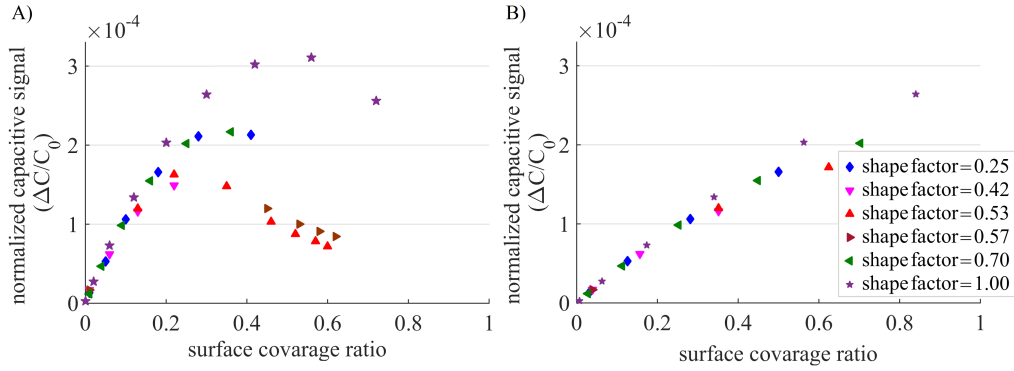

Fig. 10. The capacity change for A) $R_e/R_s = 1$ and B) $R_e/R_s = 0.6$, as a function of coverage ratio for different shape-factors of agglomeration of molecules.

have hyperbolical shapes, they clearly show how a similar coverage ratio may result in completely different capacity changes.

Figure 10 shows the normalized capacity change as a function of the coverage ratio, while considering a random circularity (and an eccentricity of zero) of the area subjected to surface stress. The graphs are obtained for two cases, namely, $R_e = R_s$ (Figure 10-A) and $R_e = 0.6R_S$ (Figure 10-B). As can be observed, the maximum capacity change occurs when the shape of the adsorption is circular, i.e. the shape factor is equal to one.

When $R_e = R_s$ (Figure 10-A), the output of the sensor has a strong dependence on the shape of the agglomeration of molecules and this leads to a significant reduction in the precision of the sensor. First of all, there is no one-to-one relationship between the capacity change and the coverage ratio. Second, a similar coverage ratio may result in a relatively large range of capacity change. Moreover, the maximum capacity change occurs when the coverage ratio is around 0.58, though, the results indicate that the precision of the sensor is the worst around this coverage ratio.

When $R_e = 0.76R_s$ (Figure 10-B), on the other hand, the response of the system has a near linear relationship with the coverage ratio and the maximum capacity change occurs with the full coverage. Reducing the size of the functionalized area can strongly confine the dependency of the capacity change to the shape of the adsorption area.

Figure 11 shows the range of the capacity change caused by different eccentricity of the aggregation of molecules. The results of the FEM simulations show that for any coverage ratio, the maximum signal occurs if the aggregation of molecules is concentric at the functionalized area (i.e. f_e is minimum or equates to zero), and this signal decreases monotonically with the eccentricity. Therefore, for a similar coverage ratio, a large range of output signal might be observed. This is only due to different eccentricities which results in a very poor accuracy and precision for the sensor (see Figure 11-A). Clearly, the maximum eccentricity can be confined by reducing the size of the functionalized area (see Figure 11-B). In fact, by reducing the size of functionalized area, the response of the sensor has a near linear and a one-to-one relation with the coverage ratio of the target molecules.

In order to clarify the effect of reducing the size of the functionalized area on the accuracy of the system, the relative range of capacitance change due to the
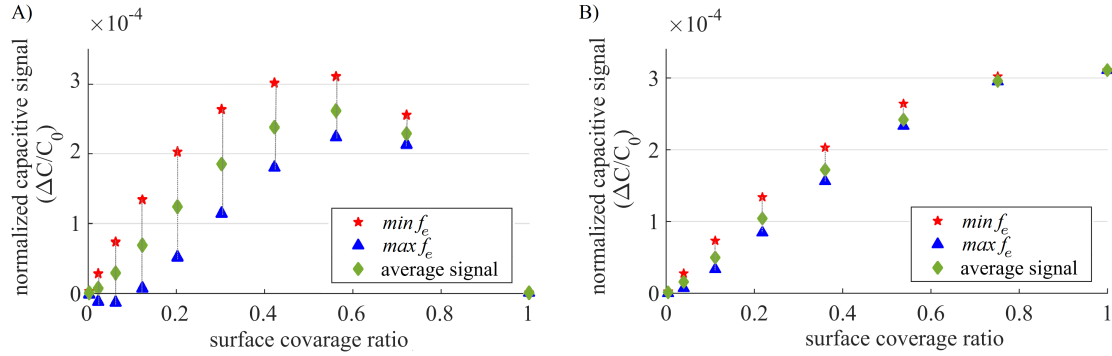
Fig. 11. The range of the output signal for A) $R_e/R_s = 1$ and B) $R_e/R_s = 0.76$ due to eccentricity of agglomeration of molecules.

eccentricity of agglomeration of molecules is shown in Figure 12. It can be clearly observed that for any radius of the functionalized area, the poorest accuracy can be expected for the lowest coverage ratio. For instance, for $R_e/R_s = 1$, when a small cluster of molecules is adsorbed to the functionalized area, the range of the response of the sensor is higher than three times its average response.

The range of the capacitive signal for any coverage ratio can be reduced to a large extent, when the size of the functionalized area is decreased, which, in turn, increases the accuracy and precision of the sensor. Evidently, this increase in the accuracy and precision is limited by the inherent *signal to noise ratio* of the sensor, in practice. Overall, the results of this study shows that by decreasing the size of the functionalized area, not only the sensitivity of the surface stress sensors can be optimized, but also, the linearity, accuracy and precision of the system can be improved.
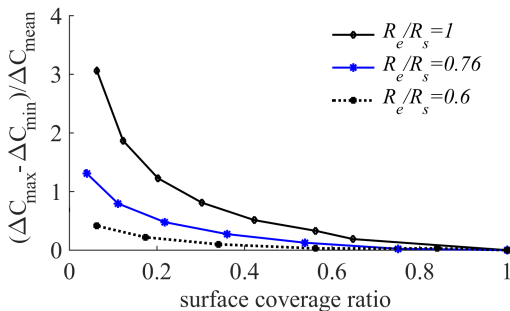

Fig. 12. The relative range of capacitance changes, due to eccentricity of agglomeration of molecules for different radii of the functionalized area.

VII. CONCLUSION

This paper presented an analytical solution for the displacement of a membrane subjected to a surface stress changes in a part of its surface. Using this solution, we derived the sensitivity of a membrane-shape capacitive sensor for surface stress measurement. The competence of the proposed solution was verified by a comparison with a detailed finite element model. The proposed analytical solution presents a very accurate, fast and robust tool that can be used for design purposes.

The results of this study imply that the relative size of the functionalized area, has a significant influence on the overall performance of such a sensor. This solution shows that we can increase the deflection of the circular membrane-shape sensor up to at least 22 percent of that of an equivalent cantilever shaped sensor. It is important to emphasize that using membrane sensors, in comparison to cantilevers, allow us to benefit from capacitive read-out techniques in liquid environments. Although the absolute amount of capacity change is small, due to the high resolution of capacitive measurements, the ultimate (optimized) sensitivity may be comparable to —or even better than— cantilevers.

Furthermore, it was noticed that using the proposed optimized size of the functionalized area, the linearity, accuracy and precision of the system can be significantly improved. Consequently, the overall reliability of the system can be increased.

References

[1] J. Tamayo, P. M. Kosaka, J. J. Ruz, A. San Paulo, and M. Calleja, "Biosensors based on nanomechanical systems," *Chemical Society Reviews*, vol. 42, no. 3, pp. 1287–1311, 2013.

[2] F. T. Goericke and W. P. King, "Modeling piezoresistive microcantilever sensor response to surface stress for biochemical sensors," *IEEE Sensors Journal*, vol. 8, no. 8, pp. 1404–1410, 2008.

[3] J. Arlett, E. Myers, and M. Roukes, "Comparative advantages of mechanical biosensors," *Nature nanotechnology*, vol. 6, no. 4, pp. 203–215, 2011.

[4] M. Godin, V. Tabard-Cossa, Y. Miyahara, T. Monga, P. Williams, L. Beaulieu, R. B. Lennox, and P. Grutter, "Cantilever-based sensing: the origin of surface stress and optimization strategies," *Nanotechnology*, vol. 21, no. 7, p. 075501, 2010.

[5] E. T. Carlen, M. S. Weinberg, C. E. Dube, A. M. Zapata, and J. T. Borenstein, "Micromachined silicon plates for sensing molecular interactions," *Applied physics letters*, vol. 89, no. 17, p. 173123, 2006. [Online]. Available: http://dx.doi.org/10.1063/1.2364878

[6] R. Raiteri, H.-J. Butt, and M. Grattarola, "Changes in surface stress at the liquid/solid interface measured with a microcantilever," *Electrochimica Acta*, vol. 46, no. 2, pp. 157–163, 2000.

[7] J.-k. Choi, M. Cha, and J. Lee, "Thin membrane transducer detectiing dna hybridization on chip," in *Sensors, 2009 IEEE*. IEEE, Conference Proceedings, pp. 815–818.

[8] A. Zapata, E. Carlen, E. Kim, J. Hsiao, D. Traviglia, and M. Weinberg, "Biomolecular sensing using surface micromachined silicon plates," in *Solid-State Sensors, Actuators and Microsystems Conference, 2007. TRANSDUCERS 2007. International*. IEEE, Conference Proceedings, pp. 831–834.

[9] M. Cha, J. Shin, J.-H. Kim, I. Kim, J. Choi, N. Lee, B.-G. Kim, and J. Lee, "Biomolecular detection with a thin membrane transducer," *Lab chip*, vol. 8, no. 6, pp. 932–937, 2008.

[10] S. Satyanarayana, D. T. McCormick, and A. Majumdar, "Parylene micro membrane capacitive sensor array for chemical and biological sensing," *Sensors and Actuators B: Chemical*, vol. 115, no. 1, pp. 494–502, 2006. [Online]. Available: http://dx.doi.org/10.1016/j.snb.2005.10.013

[11] W. Zhang, H. Feng, S. Sang, Q. Shi, J. Hu, P. Li, and G. Li, "Structural optimization of the micro-membrane for a novel surface stress-based capacitive biosensor," *Microelectronic Engineering*, vol. 106, pp. 9–12, 2013.

[12] V. Tsouti and S. Chatzandroulis, "Sensitivity study of surface stress biosensors based on ultrathin si membranes," *Microelectronic Engineering*, vol. 90, pp. 29–32, 2012.

[13] V. Tsouti, C. Boutopoulos, M. Ioannou, D. Goustouridis, D. Kafetzopoulos, I. Zergioti, D. Tsoukalas, P. Normand, and S. Chatzandroulis, "Evaluation of capacitive surface stress biosensors," *Microelectronic Engineering*, vol. 90, pp. 37–39, 2012.

[14] A. Moulin, S. O'shea, and M. Welland, "Microcantilever-based biosensors," *Ultramicroscopy*, vol. 82, no. 1, pp. 23–31, 2000.

[15] V. Tabard-Cossa, M. Godin, I. J. Burgess, T. Monga, R. B. Lennox, and P. Grütter, "Microcantilever-based sensors: effect of morphology, adhesion, and cleanliness of the sensing surface on surface stress," *Analytical chemistry*, vol. 79, no. 21, pp. 8136–8143, 2007.

[16] V. Tsouti and S. Chatzandroulis, "Non-ideal biological layer deposition effects on membrane surface stress based biosensor performance," *Microelectronic Engineering*, vol. 144, pp. 23–26, 2015.

[17] M. L. Sushko, J. H. Harding, A. L. Shluger, R. A. McKendry, and M. Watari, "Physics of nanomechanical biosensing on cantilever arrays," *Advanced Materials*, vol. 20, no. 20, pp. 3848–3853, 2008.

[18] Z. Gao, C.-S. Kim, and D. B. Henthorn, "Sensor application of poly (ethylene glycol) diacrylate hydrogels chemically-anchored on polymer surface," *IEEE Sensors Journal*, vol. 13, no. 5, pp. 1690–1698, 2013.

[19] J. Tian, Y. Bai, X. Tang, S. Sang, and F. Wang, "A capacitive surface stress biosensor for csfv detection," *Microelectronic Engineering*, 2016.

[20] G. G. Stoney, "The tension of metallic films deposited by electrolysis," *Proceedings of the Royal Society of London. Series A, Containing Papers of a Mathematical and Physical Character*, vol. 82, no. 553, pp. 172–175, 1909.

[21] X. Feng, Y. Huang, and A. Rosakis, "On the stoney formula for a thin film/substrate system with nonuniform substrate thickness," *Urbana*, vol. 51, p. 61801, 2007.

[22] Y. Huang and A. Rosakis, "Extension of stoney's formula to non-uniform temperature distributions in thin film/substrate systems. the case of radial symmetry," *Journal of the Mechanics and Physics of Solids*, vol. 53, no. 11, pp. 2483–2500, 2005. [Online]. Available: http://dx.doi.org/10.1016/j.jmps.2005.06.003

[23] L. Freund, "Substrate curvature due to thin film mismatch strain in the nonlinear deformation range," *Journal of the Mechanics and Physics of Solids*, vol. 48, no. 6, pp. 1159–1174, 2000. [Online]. Available: http://dx.doi.org/10.1016/S0022-5096(99)00070-8

[24] S. Timoshenko, S. Woinowsky-Krieger, and S. Woinowsky, *Theory of plates and shells*. McGraw-hill New York, 1959, vol. 2. [Online]. Available: https://books.google.nl/books?id=rTQFAAAAMAAJ

[25] J. Park, I. C. Kim, J. Cha, S. Park, J. Lee, and B. Kim, "Mechanotransduction of cardiomyocytes interacting with a thin membrane transducer," *Journal of Micromechanics and Microengineering*, vol. 17, no. 6, p. 1162, 2007.